

Plasma-Facing Materials Research for Fusion Reactors at FOM Rijnhuizen

J. Rapp¹, G.M. Wright², E. Alves³, L.C. Alves³, N.P. Barradas³, G. De Temmerman¹, K. Ertl⁴, J. Linke⁵, M. Mayer⁴, G.J van Rooij¹, J. Westerhout¹, P.A. Zeijlmans van Emmichoven¹, A.W. Kleyn^{1,6}

¹FOM-Rijnhuizen, EURATOM Association, Trilateral Euregio Cluster, Nieuwegein, The Netherlands

²Plasma Science and Fusion Center, MIT, Cambridge, USA

³Instituto Tecnológico e Nuclear, Sacavem, Portugal

⁴Max-Planck-Institut für Plasmaphysik, EURATOM Association, Garching, Germany

⁵IEF-2, Forschungszentrum Jülich, EURATOM Association, Trilateral Euregio Cluster, Jülich, Germany

⁶Leiden Institute of Chemistry, The Netherlands

In next generation magnetic fusion devices such as ITER, plasma-facing materials are exposed to unprecedented high ion, power and neutron fluxes. Those extreme conditions cannot be recreated in current fusion devices from the tokamak type. The plasma-surface interaction is still an area of great uncertainty.

At FOM Rijnhuizen, linear plasma generators are used to investigate plasma-material interactions under high hydrogen ion flux-densities ($\leq 10^{25} \text{ m}^{-2}\text{s}^{-1}$) at low electron temperatures ($\leq 10 \text{ eV}$), similar to the conditions expected in the divertor of ITER. The incident ion fluxes result in power fluxes of $>10 \text{ MW/m}^2$. A new linear plasma device, Magnum-PSI, is expected to begin regular plasma operations in the middle of 2011. This device can operate in steady-state with the use of a 3 T super-conducting magnet, and a plasma column diameter projected to 100 mm. In addition, experimental conditions can be varied over a wide range, such as different target materials, plasma temperatures, beam diameters, particle fluxes, inclination angles of target, background pressures, magnetic fields, etc., making Magnum-PSI an excellent test bed for high heat flux components of future fusion reactors.

Current research is performed on a smaller experiment, Pilot-PSI, which is limited to pulsed operation, a maximum magnetic field of 1.6 T and a narrow ($\sim 20 \text{ mm}$) column width. The research is primarily focused on carbon based materials and refractory metals. Erosion of materials, surface morphology changes as well as hydrogen implantation, diffusion and inventory in the materials are studied under fusion reactor conditions. The influence of neutron damages is studied by irradiation of the materials with high energy ions.

An overview of the results obtained on Pilot-PSI with respect to carbon erosion, hydrogen retention in refractory metals and transient heat loads is presented.

Introduction

The ITER divertor will experience ion fluxes of $10^{24} \text{ m}^{-2} \text{ s}^{-1}$ and steady-state power fluxes of 10 MWm^{-2} [1]. In addition transient heat loads will occur. A reasonable lifetime of the divertor demands that those transient heat loads will be limited to $44 \text{ MJm}^{-2}\text{s}^{-1/2}$ [2]. Those power fluxes are achieved in the so-called partially detached divertor operation, which leads to divertor plasmas with very high densities and low electron temperatures (1-10 eV). Those plasma facing components conditions are un-precedented and require new dedicated experimental facilities to test target materials and components under those conditions. Magnum-PSI (MAgnetized plasma Generator and NUMerical Modelling) was designed to explore this divertor plasma regime. Magnum-PSI (see figure 1) is a linear plasma generator with a steady-state 3 T magnetic field [3]. The plasma is produced by a cascaded arc source [4] delivering 10 MWm^{-2} steady-state power fluxes in a plasma jet of 10 cm diameter to the target. In addition this plasma source can be pulsed superimposed to the steady-state hydrogen plasma delivering transient heat flux densities of about 2 GWm^{-2} for a duration of 0.5 ms. There are numerous other devices, which can simulate those transient heat fluxes [5-8].

However those devices do not combine the simultaneous exposure of the target by the ITER-relevant steady-state as well as transient ion fluxes.

Current research is performed on a smaller experiment, Pilot-PSI, which is limited to pulsed operation, a maximum magnetic field of 1.6 T and a narrow (~ 20 mm) column width. Pilot-PSI has already achieved in many aspects the ITER-like conditions. Figure 2 shows the operational space of Pilot-PSI together with the ITER parameter range for the divertor and the first wall. The plasma parameters were measured by Thomson Scattering in front of target [9]. Very high ion fluxes in excess of $10^{25} \text{ m}^{-2}\text{s}^{-1}$ were achieved on the target (at normal field line incidence) at low electron temperatures and high electron densities [10]. Those plasma conditions are comparable to the plasma conditions at the strike point of the outer divertor in ITER. At lower electron densities ($n_e < 10^{21} \text{ m}^{-3}$) electron temperatures of 5 eV have been reached. This is a demonstration that the first 5cm from the strike point into the Scrape-Off-Layer (SOL) on the outer vertical target of ITER can be simulated in Magnum-PSI in which the target can be tilted with respect to the magnetic field to similar field line angles as in ITER. Large targets with sizes of up to 60×12 cm and weight of 100 kg can be exposed in Magnum-PSI. It is planned to increase the plasma temperature to 10 eV by radio-frequency heating [11,12]. In addition ion energies of almost 100 eV were reached by biasing the target so that also the plasma surface interaction in-front of the first wall components in ITER can be re-created in Pilot-PSI and Magnum-PSI.

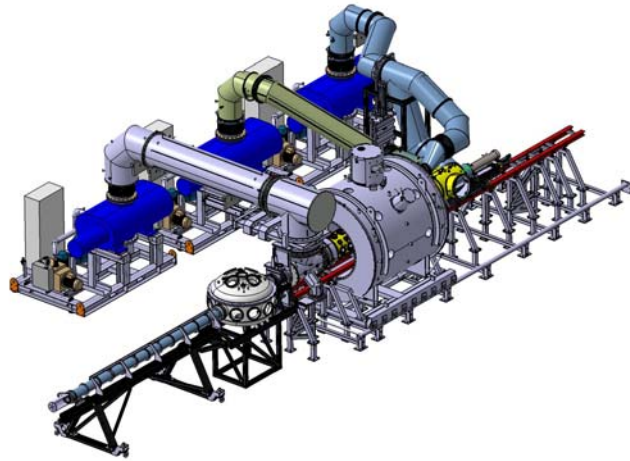


Fig. 1: Magnum-PSI

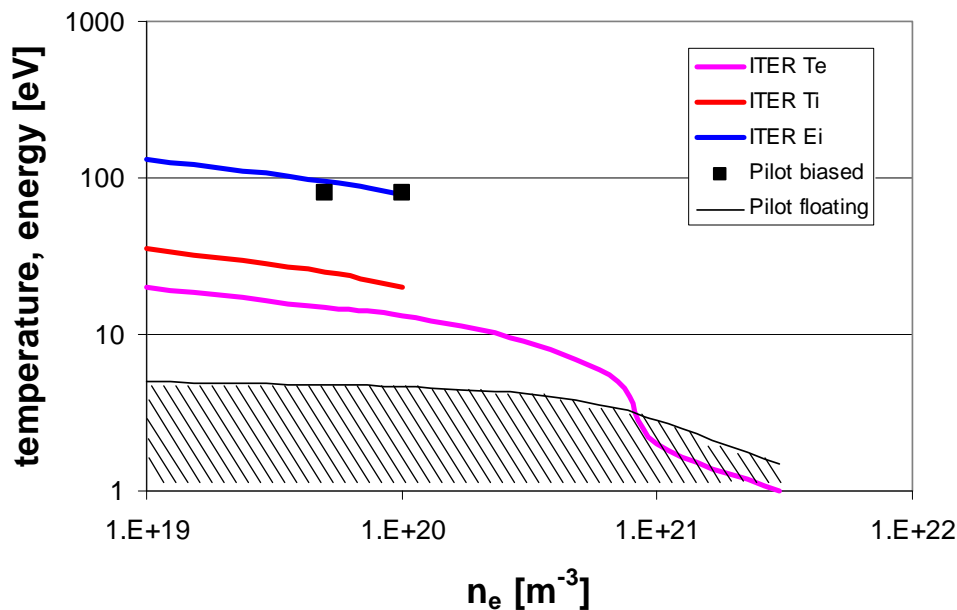


Fig. 2: Operation domain of Pilot-PSI (in black and hatched area) and ITER edge operation domain.

Research on Pilot-PSI is primarily focused on carbon based materials and refractory metals. Erosion of materials, surface morphology changes as well as hydrogen implantation, diffusion and inventory in the materials are studied under fusion reactor conditions. An overview of the results obtained on Pilot-PSI is given.

Carbon chemical erosion investigations

Carbon chemical erosion is often measured in-situ by optical emission spectroscopy. The spectroscopy on the molecular CH A-X Gerö band makes it possible to quantify in situ the chemical erosion of carbon wall elements in contact with hydrogen plasma. CH is the only hydrocarbon that is accessible by emission spectroscopy in the visible. CH spectroscopy relies on the correlation between CH radiation and methane particle fluxes, the main reaction product formed upon chemical erosion of carbon. The method is widely applied in fusion experiments and provides insight that is presently used to make predictions for ITER

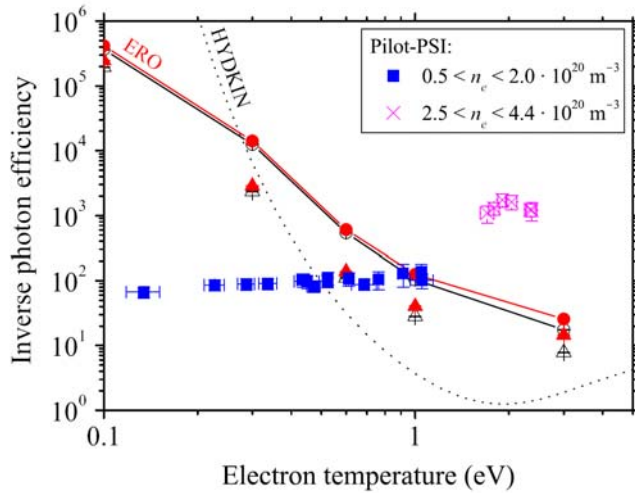


Figure 3: Inverse photon efficiency (D/XB) for CH emission from CH₄ injection experiments, comparison to ERO and Hydkin calculation.

and temperatures 1–10 eV. Due to steep gradients in the rate coefficients that govern the relation between the CH radiation and the chemical erosion, it is generally regarded as impossible to apply the existing methodology to plasma temperatures below ~3 eV.

We demonstrated that the interpretation of the spectroscopic data has to be revised for these high density low temperature plasmas on the basis of experiments in the linear plasma generator Pilot-PSI.

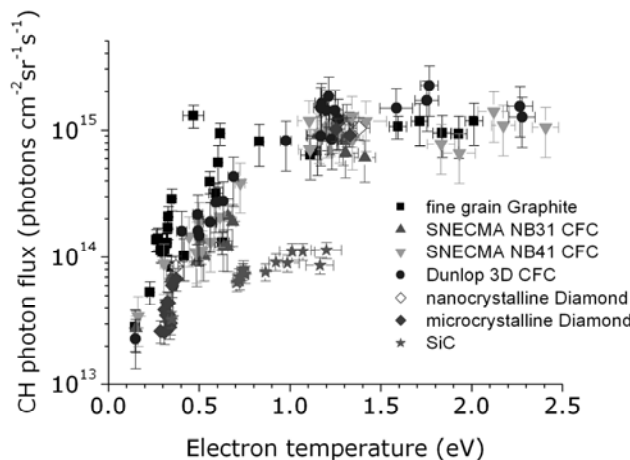


Figure 4: CH photon flux as a function of plasma electron temperature in the range 0.1-2.5 eV for a range of carbon-based materials.

plasma wall issues. Also for ITER it would be an obvious diagnostic. This requires, however, that it has to be applied in the extreme and unexplored plasma regime of densities $>10^{20} \text{ m}^{-3}$

Also for ITER it would be an obvious diagnostic. This requires, however, that it has to be applied in the extreme and unexplored plasma regime of densities $>10^{20} \text{ m}^{-3}$

Methane was injected in plasma of electron temperature $T_e = 0.1-2.5 \text{ eV}$ and electron density $(0.5-5) \times 10^{20} \text{ m}^{-3}$. Calculated inverse photon efficiencies for these conditions range from 3 up to $>10^6$ due to a steeply decreasing electron excitation cross section. The experimental results contradicted the calculations made with HYDKIN and ERO [13,14] and show a constant effective inverse photon efficiency of ~ 100 for $T_e < 1 \text{ eV}$ (see figure 3). The

discrepancy is explained as the CH A level is populated through dissociative recombination of the molecular ions formed by charge exchange. These

results form a framework for in situ carbon erosion measurements in future fusion reactors such as ITER.

The high ITER-like fluxes have been exploited to perform experiments on the chemical erosion of carbon [15]. One of the key open questions of chemical erosion is the yield dependence on T_e . It is not clear how quickly carbon will chemically erode in the high-density, low-temperature plasma that is expected in a detached ITER divertor. With the Pilot-PSI experiment, the gross erosion yields under these conditions can be measured directly. Results from plasma exposure to high-flux ($>10^{23}$ H^+/m^2s) and low-temperature hydrogen plasma (see figure 4) indicate silicon carbide (SiC) has a lower relative rate of gross erosion than other carbon-based materials (fine-grain graphite (FGG), ITER-grade CFC (NB31, NB41 and Dunlop 3-D)) by a factor of ~ 10 . Pyrometry and literature indicates this lower gross erosion yield of SiC is not a surface temperature effect. Literature shows that total (Si and C) gross erosion of SiC is a factor of 4-5 lower than for pure carbon at low ion energies (20 eV) for temperatures up to 1100 K [16], which, when taking into account the factor of 2 lowering of CH photon flux from Si content in the SiC, is in good agreement with our spectroscopic measurements. So it would appear that the reduced erosion rate seen for SiC can be attributed to a physical property of the material rather than changing experimental conditions for these exposures. Similar lower erosion yields have been obtained with diamond targets (nanocrystalline (NCD) and microcrystalline (MCD) diamond coated graphite). The indications from this study are that the best choice from an erosion and lifetime perspective, for a carbon-based material as a divertor plasma-facing component in future fusion devices, would be SiC or diamond.

Hydrogenic retention in refractory metals

Laboratory results have established that hydrogenic retention of the refractory metals tungsten (W) and molybdenum (Mo) is very low. However, these laboratory experiments do not take into consideration many factors that will play a role in future fusion devices such as high ($>10^{23}$ $m^{-2}s^{-1}$) ion fluxes, neutron irradiation and thermal stressing resulting in surface cracking. The linear plasma generators at FOM Rijnhuizen allow us to examine the impact of high plasma fluxes on the hydrogenic retention of these low solubility metals.

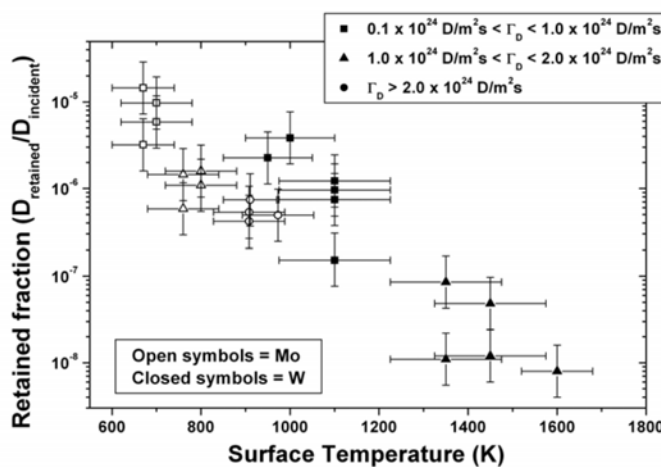


Figure 5: Retained fraction from various locations on a W and Mo target exposed to 80s Pilot-PSI plasma.

Hydrogen retention in refractory metals like Mo and W has been studied extensively in Pilot-PSI [17]. The main indication from these results is that W and Mo targets retain very little D when compared with the amount of D incident to the surface ($D_{retained}/D_{incident} \sim 10^{-8}-10^{-5}$). The W results show no clear dependence of retention on incident fluence. It appears that the hydrogen retention is mainly a function of the surface temperature (see figure 5), making those metals attractive plasma facing components for future fusion reactors beyond ITER, which will most likely operate with hot walls.

However, in future fusion reactors there will be other factors that may affect hydrogenic retention and may also be modified by high plasma fluxes. Primarily, this is the presence of 14.1 MeV neutrons from the deuterium-tritium fusion reaction. These energetic neutrons can displace lattice atoms as they pass through the material and this damage leads to creation of trap sites. In this work, heavy ions are used to create these displacements due to time and safety constraints working with neutron-irradiated materials [18]. W targets (as received and unannealed) were irradiated at 300 K with 12.3 MeV W^{4+} ions. Using W ions prevents any side effects from implantation of impurity species into the lattice, however, the damage is confined to the penetration depth of the W ion ($\sim 1.5 \mu\text{m}$ for 12.3 MeV W^{4+}) as opposed to evenly distributed throughout the material as one would expect with neutron irradiation. A range of damage levels were investigated ranging from 0.5-10 displacements per atom (dpa) and compared to un-irradiated tungsten. The targets were then exposed to high flux deuterium plasmas in Pilot-PSI with one set of irradiated targets exposed at low surface temperatures ($T_W < 500 \text{ K}$) and one set exposed at high surface temperatures ($650 \text{ K} < T_W < 1000 \text{ K}$). NRA results show a clear enhancement of retention due to the heavy-ion irradiation (see figure 6), but the enhancement is not dependent on the dpa level in the target, implying any enhancement effects are saturated at a dpa level of 0.5 dpa. Higher surface temperatures during plasma exposure ($T_W > 900 \text{ K}$) correspond to the greatest enhancement of retention. Low surface temperatures ($T_W < 500 \text{ K}$) result in low enhancement for these exposures due to the low diffusion rates of the implanted deuterium and limited access to the $1.5 \mu\text{m}$ damage

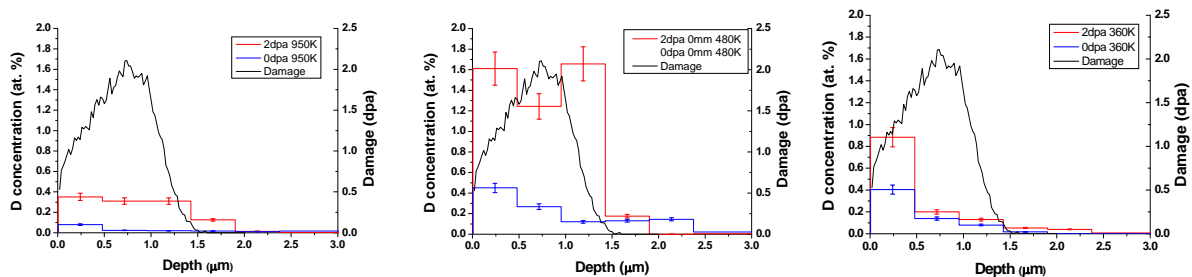


Figure 6: D retention in W; deuterium concentration profiles for different surface temperatures (NRA)

range for the 80 s exposure time. Longer exposure times are used to investigate the fluence/time dependence of retention for the low surface temperature exposures. Trap concentrations as high as 1.5 at.% were measured. The enhancement of the retention as compared to un-irradiated targets ranges from a factor of 2-20.

TMAP7, a 1-D slab diffusion code, has been used to analyze the Thermal Desorption Spectroscopy (TDS) data from the high temperature plasma exposures and low temperature plasma exposures of pre-irradiated targets in Pilot-PSI. The analysis indicates that the damage from the 12.3 MeV W^{4+} irradiation has led to the production of at least three distinct trap types in the tungsten lattice. Comparing the fit trap energies and desorption peak positions to literature, it is likely the irradiation is producing a mixture of dislocations, vacancies, and vacancy cluster in the tungsten lattice. TDS spectra show us that the irradiation is creating two types of defects in the W that are influence the hydrogenic retention. The lower temperature desorption peaks (500–600 K) likely represent single vacancies with a trap energy of 1.0–1.4 eV. The high-temperature desorption peak (850 K) is likely associated with the formation of microvoids or vacancy clusters in the W with a trap energy of $\sim 1.7 \text{ eV}$. It is these high-energy traps that contribute significantly to the retention at high surface temperatures during the plasma exposure.

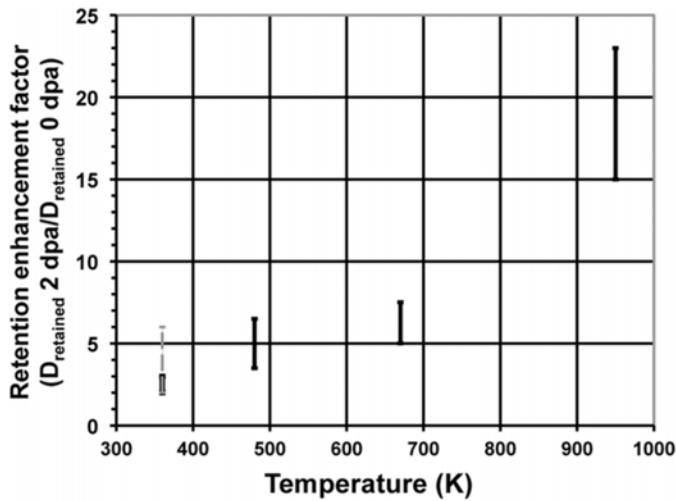


Figure 7: Retained fraction from various locations on a W and Mo target exposed to 80s Pilot-PSI plasma.

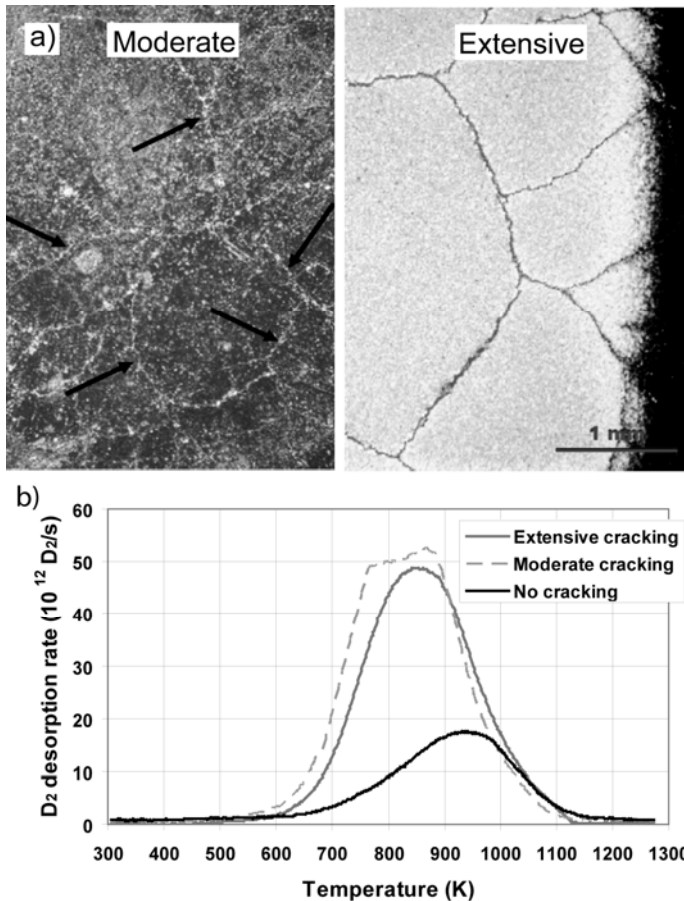


Figure 8 a) SEM images of W targets with “moderate” and “extensive” surface cracking due to thermal cycling via e-beam irradiation. b) TDS spectra for thermally-stressed W with various degrees of surface cracking and exposed in Pilot-PSI.

Plasma-facing materials in future fusion reactors will also experience high thermal stresses both from steady-state heat loads (≤ 30 MW/m²) and transient events such as ELMs (≤ 1 GW/m²). These thermal stresses can lead to extensive cracking of the surface. It is unclear the impact this cracking has on hydrogenic retention properties. In this investigation, W targets were exposed to high thermal heat loads in the JUDITH e-beam facility which resulted in cracking of the surface. The targets with surface cracking were then exposed to high flux deuterium plasma in Pilot-PSI as well as a reference target with no prior thermal stressing in JUDITH.

TDS analysis was used to determine the retention properties of these different surface conditions. From the TDS profiles it is clear that the lower temperature desorption peaks seen on the irradiated W targets are not present meaning the lower energy traps have been removed from these targets. Comparison of the TDS results (see figure 5) reveals that the thermally-stressed W has a total retention a factor of 2.1 ± 0.2 higher than the unstressed W. Some or perhaps all of this difference could be attributed to the slightly higher surface temperature during plasma exposure for the unstressed W ($T_{\text{surf}} \sim 1150$ K) than for the thermally-stressed W ($T_{\text{surf}} \sim 1100$ K). Although a 50 K difference in surface temperature may not seem like a large difference, we see this is in a region with strong temperature dependence on surface temperature. It is important to note that the difference in hydrogenic retention between the moderate cracking and extensive cracking scenarios is negligible. This indicates that any enhancement

of retention is not related to the physical manifestation of the thermal stressing (i.e. cracking, surface roughening) but rather through the introduction of thermal defects in the lattice that enhance the retention.

Transient heat load to simulate ELMs in a linear device

A pulsed-plasma source [19] is being developed for the study of the effect of transient heat loads on the plasma-exposed surface, with the aim of simulating what would happen during Edge Localized Modes (ELMs) in ITER. The cascaded arc is coupled to a capacitor bank in parallel to its power supplies for the steady state operation. The capacitor bank is discharged

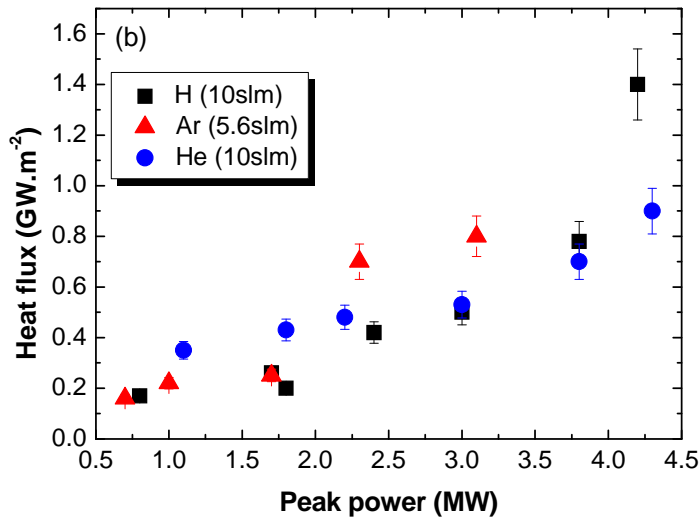


Figure 9: Peak heat flux to the target during transient (0.5 ms) pulsing of the cascading arc in Pilot-PSI.

during the steady state operation and produces a transient power increase in the source. This leads to a sudden rise of the plasma density and temperature for duration of about 0.5 ms. The time duration can be adjusted by an inductance in the circuit. Transient discharge currents of up to 9 kA were reached. The increase of power to the plasma mainly increases the ionization of the plasma and hence the plasma density. This led to record plasma densities in excess of $1.2 \times 10^{22} \text{ m}^{-3}$ and electron temperatures of up to 6 eV. This translates into peak heat flux densities of 1.4 GWm^{-2} on the target. Those were determined by the plasma parameters in front of the target and IR thermography. The evolution of the surface temperature

during such a pulse is very similar to those found in tokamaks during ELMs.

Summary

Pilot-Psi the forerunner experiment of Magnum-PSI has demonstrated performance compatible with the plasma conditions as they will occur in front of the plasma facing components in future fusion reactors. Carbon based targets as well as refractory metal targets (W and Mo) were exposed to those plasma. Since tungsten is the prime candidate as plasma facing material of future fusion reactors it was investigated in detail in Pilot-PSI already. The Deuterium retention in this refractory metal was found to be low $<10^{-4}$. However, damaged tungsten targets experience higher Deuterium retention. Stress damage was found to increase the Deuterium retention by a factor of. Neutron damage of the material was found to have even a more profound effect. At high target temperatures, when Deuterium diffusion in the bulk of the tungsten material is high, an enhancement of the Deuterium retention (when compared to undamaged targets) of up to a factor of 20 was observed. In addition to those prime target materials novel materials like SiC and diamond were tested. The chemical erosion of SiC and diamond proved to be significantly lower than that of other ordinary carbon based materials (graphite, CFCs).

Acknowledgements

This work, supported by the European Communities under the contract of Association between EURATOM/FOM and carried out within the framework of the European Fusion Programme with financial support from NWO and NWO grant No. RFBR 047.018.002. The views and opinions expressed herein do not necessarily reflect those of the European Commission.

- [1] G. Federici, et al. (2001) Nucl. Fusion **41** 1967.
- [2] P.R. Thomas, IT/1-5 22nd IAEA Fusion Energy Conference (Geneva, 13-18 October 2008).
- [3] J. Rapp, et al., Fus. Eng. Des., published online
<http://www.sciencedirect.com/dx.doi.org/10.1016/j.fusengdes.2010.04.009>
- [4] M.C.M. van de Sanden, et al. (1992) Rev. Sci. Instrum. **63** 3369.
- [5] M.A. Bourham, et al. (1989) IEEE Transactions on Plasma Science **17** 386.
- [6] T. Hirai, et al. (2007) Phys. Scr. **T128** 166.
- [7] I.E. Garkusha, et al. (2009) Phys. Scr. **T138** 014054.
- [8] S. Kajita, et al. (2007) Nucl. Fusion **47** 1358.
- [9] H.J. van der Meiden, et al. (2008) Rev. Sci. Instrum **79** 13505.
- [10] G.J. van Rooij, et al. G.J. (2007) Appl. Phys. Lett. **90** 121501.
- [11] R. Koch, et al. (2005) Trans. of Fus. Science Techn. **47** 249-251.
- [12] R. Koch, et al. (2007) AIP Conf. Proc. Radio Frequency Power in Plasmas **933** 517-520.
- [13] J. Westerhout, et al., (2009) Appl. Phys. Lett. **95** 151501.
- [14] J. Westerhout, et al., (2010) Nucl. Fusion **50** 095003.
- [15] J. Westerhout, et al., (2009) Phys. Scr. **T138** 014017.
- [16] M. Balden, S. Picarle, J. Roth, J. Nucl. Mater. 290-293 (2001) 47.
- [17] G.M. Wright, et al., (2010) Nucl. Fusion **50** 055004.
- [18] G.M. Wright, et al., (2010) Nucl. Fusion **50** 075006.
- [19] G. De Temmerman, et al., (2010) Appl. Phys. Lett. **97** 081502.